Polym. Bull. (2009) 62:355–366
DOI 10.1007/s00289-008-0024-9

ORIGINAL PAPER

# Synthesis and study of photoacoustic properties of ($Pd/TiO_2$)/polystyrene nanocomposites

**M. F. Meléndrez Castro · G. Cárdenas Triviño · J. Morales · J. Díaz Visurraga · C. Cruzat Contreras**

Received: 5 September 2008 / Revised: 25 October 2008 / Accepted: 30 November 2008 /
Published online: 11 December 2008
© Springer-Verlag 2008

**Abstract** In this work, nanocomposites (Ncs) from Pd nanoparticles and $TiO_2$ (Pd-Nps-$TiO_2$) were supported on a polystyrene matrix (PS). Chemical liquid deposition, solvated metal atom dispersion and in situ polymerization were used in order to synthesize these Ncs. Colloid and nanocomposite characterization were performed by TEM, SEM, EDX, SAED and TGA. TEM analysis revealed a particle size of 7 nm for Coll-Styrene and 11 nm for Pd-Nps supported on $TiO_2$ after radical polymerization. SAED showed phases corresponding to both metallic Pd and $TiO_2$ anatase in the polymeric matrix. Molecular weight (MW) was determined by viscosimetric method. MW varies according to the initiator concentration and nanoparticle amount used for polymerization. The amount of nanoparticles increased the decomposition temperature of the Ncs by 10 °C, improving the thermal stability of these hybrid materials. Photoacoustic properties were evaluated in order to determine the effect of nanoparticles on thermal diffusivity ($\alpha$) inside the matrix. Significant values of ($\alpha$) were found for Ncs with Pd-Nps in contrast to PS and $Pd/TiO_2$ Ncs. Structural aspects and colloidal aggregation of Ncs were also studied.

**Keywords** Nanocomposites · Photoacoustic properties · Colloids · Polystyrene matrix

M. F. Meléndrez Castro · G. Cárdenas Triviño (✉) · J. Díaz Visurraga · C. Cruzat Contreras
Polymers Department, Advanced Materials Laboratory,
Universidad de Concepción, Casilla postal 160-C, Concepción, Chile
e-mail: galocardenas@udec.cl

M. F. Meléndrez Castro
e-mail: mmelendrez@udec.cl

J. Morales
Photoacoustic Laboratory, Department of Physics, Faculty of Physical Sciences,
Universidad de Concepción, Concepción, Chile

## Introduction

Inorganic/polymer nanocomposites (Ncs) are of great interest because of their combined properties of both inorganic nanoparticles and organic molecules [1]. Several methods have been used to prepare polymer Ncs such as sol–gel reactions [2–4], intercalative polymerization [5–7], melt-processing [8–10], in situ polymerization [11, 12] and emulsion polymerization [13, 14] among others. Depending on the nature of nanoparticles and the synthesis/processing of polymeric matrices, the most important factors in the preparation of nanomaterials with enhanced performance include the uniform distribution of inorganic nanoparticles within the polymer matrix and the strong interfacial adhesion between both matrices and nanofillers. Another important method for the preparation of Ncs is the chemical liquid deposition with further polymerization [15, 16]. This method has been extensively used for preparing polystyrene, polymethyl metacrylate, and Ncs as well as for some copolymers with several metals (Pd, Cu, Ag, Au, Fe, Ga, Ge and Sb) [17]. This method consists of the formation of metallic colloid with the monomers before polymerization, which is elaborated by the co-deposition of metallic atoms at 77 K with monomer vapors. The latter stabilizes the metallic nanoparticles, obtaining stable colloids. Ncs obtained from this technique present a narrow size distribution of the nanoparticles, between 2 and 6 nm, with good thermal and conductive properties [18].

Nowadays, filled polymers are widely used in many fields of technology. Polymers containing semiconductor particles play significant roles, especially for the manufacturing of electronic devices [19]. Metal-polymeric Ncs are now widely used as drug carriers, magneto-optical media, magnetic liquids, and for information recording films. In particular, organic–inorganic hybrid composites [20–22] are very promising photonic materials for optical data storage, optical waveguides, sensors, electrochromic smart windows, solid-state lasers and screen displays, as well as for other supramolecular and photonic systems and devices [23–25]. Colloidal surface engineering is a current topic of applied chemistry in the field of developing new materials. Composite colloidal particles (core-shell structures) have several expected applications in the area of coatings, electronics, photonics and catalysis [26].

Extensive studies of NCs and PS introduced on carbon nanotubes [27], metallic nanoparticles [28], oxides [29, 30] and semiconductor materials such as CdSe, PbS, HgS, $MoS_2$, GaP, $TiO_2$, $SiO_2$ and $Fe_2O_3$ have been developed [31–36]. Current research in NCs are focused on the enhancing of barrier, thermal and mechanical properties of the polymers, however, the application of the interesting properties of nanomaterials have not been exploited for the elaboration of last generation materials.

This work presents the preliminary results of the preparation of Pd–$TiO_2$ Ncs supported on a PS matrix. Synthesis was conducted by chemical liquid deposition (CLD) in order to obtain Pd colloidal nanoparticles with styrene (Pd-Coll-Styr). Colloidal nanoparticles were supported in situ on the semiconductor oxide, and it was polymerized using AIBN as an initiator. Thermal and photoacoustic studies were performed in order to determine the thermal diffusivity ($\alpha$) of obtained Ncs. ($\alpha$) is a measure of rate at which a temperature disturbance at one point in a body travels to another point and it is related to energy flow with gradients. This parameter is

affected by the amount and kind of material incorporated into the polymeric matrix. High values of thermal diffusivity can facilitate the combination process in sensor particles ($Pd/TiO_2$) in gaseous media, increasing their efficiency on gas detection. Structural and morphological parameters, colloid stability studies and thermal properties are also discussed in this paper.

## Experimental

### Synthesis

Pd-Colls were prepared by CLD method [37], which involves the physical vapor deposition of Pd metallic in organic media. The reaction was carried out in a glass reactor. A W-$Al_2O_3$ crucible loaded with Pd was assembled in the metallic atom reactor and the whole system was evacuated. A glass device with styrene (Fisher Co., USA) dried and degasified by standard freeze–thaw procedure [37] was attached to the neck of the reactor. The whole system was immersed in liquid nitrogen (77 K) and evacuated at vacuum ($10^{-5}$ bar). The crucible was heated at 40 A until Pd boiling point. In the reaction, Pd metallic and the styrene were co-deposited for half an hour. The frozen matrix obtained on reactor walls, was slowly warmed for 1 h. Then, the reactor was filled with extra pure nitrogen. After 30 min under nitrogen flow, a Pd-Styr colloidal dispersion was obtained. A similar procedure was conducted with 2-propanol p.a. grade rather than styrene in order to compare the features of both media. In a typical reaction, $1.14 \times 10^{-5}$ mol of Pd metallic (Aldrich, USA) was evaporated with 100 ml of styrene. After, Pd colloidal nanoparticles were supported on $TiO_2$ anatase (1% w/w and 5% w/w) by SMAD method [38] for 24 h in inert atmosphere with constant stirring. $TiO_2$ was introduced in the reactor in order to directly support the Pd nanoparticles after monomer melt temperature and to avoid oxidation of the Pd-Nps.

### Polymerization

($Pd/TiO_2$)/Styrene (10 ml) was placed in each of the four polymerization flasks with 0.1, 1.0 mol% of AIBN, under nitrogen flow. The flasks were closed and placed in an isothermal bath at 65 °C for 9 h. The content of each flask was poured into beakers with methanol. The black Ncs obtained were filtered and dried under vacuum ($10^{-3}$ Torr) for 48 h at 50 °C. The yield of each polymeric fraction was determined. Viscosity average and molecular weight (MW) was calculated from the Mark–Houwink equation [39]. The intrinsic viscosity was measured at 25 °C on an Ostwald viscometer. Polymers were dissolved in benzene at 25 °C, $K = 11.6 \times 10^{-5}$ dL/g, $a = 0.72$ [40].

### Thermogravimetric analysis

Thermogravimetric analyses were performed on a Perkin Elmer TGA 7 Thermogravimeter Analyzer. All experiments were carried out in a nitrogen atmosphere. All

specimens were weighted in the range of 3–5 mg and heated to 550 °C at a rate of 10 °C $min^{-1}$.

Electron microscopy studies

Particle size for colloidal dispersions and Ncs were obtained from histogram analysis of TEM micrographs. A transmission electron microscope JEOL–JEM 1200EXII with 4 Å resolution was used. A drop of each colloid was placed on a dry Ni-grid (150 mesh) previously coated with carbon, in an inert atmosphere. The measure of the particle size population diameter was randomly chosen and obtained data were represented by a histogram. Therefore, the average particle size was fitted to both normal and Gaussian curves.

Determination of thermal diffusivity by photoacoustic methods

The experimental arrangement includes, as a heating source, a 250 W halogenous lamp, in which the polychromatic out-beam is mechanically modulated in intensity with the aid of a SRS-540 chopper from Stanford Research Systems [41]. The out-beam is guided towards the cell, where the rear part of the sample is illuminated. Transmission heating configuration was used (rear incidence). The cell has an aluminum body with an electret microphone fixed to every one of the walls. Voltage of the exit signal *S* of the microphone was measured by means of a SRS-850 lock-in amplifier connected to a computer. As a sample holder Teflon rings of $\sim 1-5$ mm thick and 6 mm inner diameter were used. The sample holder was adhered with vacuum grease and hermetically sealed to the cell. PA signal measurements were carried out as a function of the chopping frequency in the range of of $\sim 1-5$ mm thick and 6 mm inner diameter because under such conditions, the aluminum holder is thermically thin. Samples considered for measurements had a thickness between 600 and 800 μm. Measurements of the PS, Pd/PS-NCs y (Pd/$TiO_2$)/PS-NCs were also taken.

## Results and discussion

Black colloids were obtained in the dispersions with styrene and palladium. The reaction scheme of colloid formation (coll) and Ncs in PS matrix is shown in Fig. 1. The particle size was controlled by the concentration of metal evaporated mols and the isolation time of the frozen matrix (monomer-metal). This time rules the nucleation process of the particles and, in some cases, their structure [42]. A stability study was performed in order to determine the time at which the particles remain in suspension before flocculation. Thus, they were incorporated into the semiconductor oxide in order to avoid the support of Pd aggregated particles with sizes larger than the disperse particles. Data from Table 1 shows that Pd-Coll-2-propanol are more stable than Pd-Coll-styrene with a stabilization time of 120 h. On the other hand, Pd-Coll-styrene is very unstable and it flocculates at 2 h after its preparation. This instability is produced by the high reactivity of a large fraction of

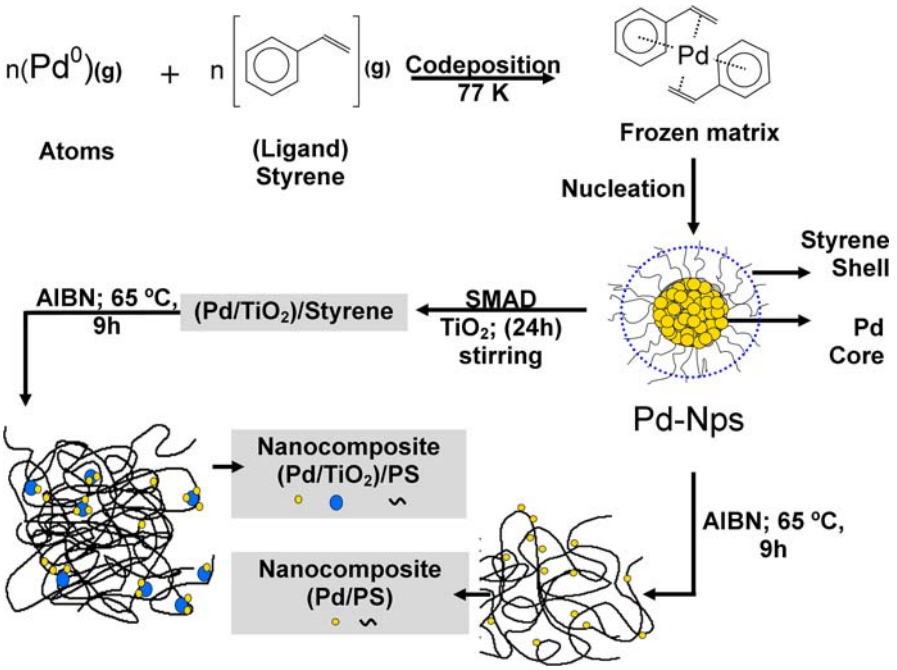


**Fig. 1** Pd-colloid and nanocomposites formation

Pd-Nps on the surface [43] and the low coordination of Pd-Nps (more reactive than bulk atoms). Therefore, the interaction between ligands (styrene or 2-propanol) should form adducts with the metal of the core-shell type to avoid interaction between particles and thus increasing the colloid stability.

A statistical study of TEM images was carried out for each colloidal system. This study consisted of the size (diameter) measurement of about 100 particles for the TEM images of the Pd-Colls, using the (TEM software Digital Micrograph (DM)$^{TM}$ 3.7.0 by Gatan Inc.) software. The counts were then plotted as frequency histograms using the Microcal$^{TM}$ Origen 6.0 software of (Microcal Software, Inc.). The mean particle sizes and standard deviation were also calculated.

Pd-Coll-2-propanol presented a lower particle size than Pd-Coll-styrene for $7 \times 10^{-4}$ mol/L. The higher particle size and the interaction between particles increase the trend of flocculation of the colloidal dispersions by strong gravity effects, such as colloids with styrene. Several CLD studies reported the synthesis of nanoparticles and colloids with monomer ligands such as MMA, ethylmethacrylate, buthylmethacrylate and styrene. Lower particle sizes (2.2–5.0 nm) [17, 44, 45] and higher stability were obtained with acrylates by the formation of bidentate interactions with the metal surface. Nps were also obtained by CLD with 2-propanol, with sizes between 2.0 and 4.0 nm. [42]. The CLD methodology presents a good reproducibility only if the synthesis parameters (evaporation conditions, colloid concentration, solvent degasification and latency time) remain constant [46]. Figure 2 presents TEM micrographs for palladium colloids obtained with both

**Table 1** Stability and particle size of Pd colloidal dispersions with 2-propanol and styrene

| Metal | Solvent | Concentration mol/L ($10^{-4}$) | Stability (h) | Particle size (nm) | Particle size supported (nm) |
|---|---|---|---|---|---|
| Pd | 2-propanol | 7.172 | <120 | 6.24 | – |
| | | 3.432 | <120 | 5.90 | – |
| | | 1.143 | <120 | 6.51 | 8.00 |
| | Styrene | 7.80 | Flocule | 7–42 | – |
| | | 3.435 | 2 | 7.34 | – |
| | | 1.143 | 2 | 7.1 | 11.10 |

styrene and 2-propanol. SAED analysis allowed us to determine the corresponding phases to Pd (111), (002), (022) and Pd (224) by comparison with the reference data [47].

An increase in Pd-Nps size was noted after the SMAD process. The size increase can be attributed to clusterization of particles supported on the oxide surface. Figure 3 shows an EDX spectrum for the Pd-Nps supported in $TiO_2$. This analysis was carried out using a JEOL–JEM 1200EXII which has a EDAX detector, the samples were tilted 45 °C in situ in the microscope to perform the EDX analyses. The Ni peaks are attributed to Niquel grid and the peaks at 4.4 and 5.1 eV correspond to Titanium Ti(K$\alpha$) and Ti($\beta$) of the $TiO_2$. The $Pd_{(L\ell)}$ signal close to 2.9 eV, confirmed the presence of palladium. The small intensity of Pd signal compared with those of Ni and Ti is due to the small amount of palladium present in the samples.

Polymerizations with Pd-Coll-Styrene were performed before the SMAD process because styrene colloids do not flocculate. Radical polymerization using AIBN as an initiator was carried out. The yield for the obtained NCs are reported in Table 2. Good yielding percentages were observed (96.4–85.9%). Incorporation of Nps-Pd and $Pd/TiO_2$ to the monomer decreases yielding percentage. These values are different from those reported by Cárdenas et al. [17] for Pd-Styrene-co-Ethylmetacrylate-NCs, which were synthesized by CLD, depositing Pd atoms and monomers post-polymerization. Yielding values of 35.40 and 27.93% using 0.1 and 1.0 mol%, respectively, were obtained. Average viscosimetric MW (Mv) values of NCs-1 to NCs-6 were compared and it was shown that the incorporation of Pd-Nps into the matrix decreases the Mv. It is probable that palladium atoms produce styrene hydrogenization, decrease the growth of macro-radicals formed or compete with the initiator radicals, originating lower MWs. These effects are more significant for the $Pd/TiO_2$ with the incorporation of $Pd/TiO_2$ and the Mv decreased from $13.83 \times 10^4$ g/mol to NCs-6. Similar behaviors are reported by Cárdenas et al. [44].

After polymerization, the Pd-Nps agglomerate and distribute in a slightly uniform way along the polymeric matrix.

TEM micrographs (Fig. 4) show that the interaction between Pd and support occurs by Pd-Nps fractal aggregates, rather than individual particles. It is probable that the polymerization temperature and formed radical amount along the matrix affects the interaction between particles previously supported on the SMAD

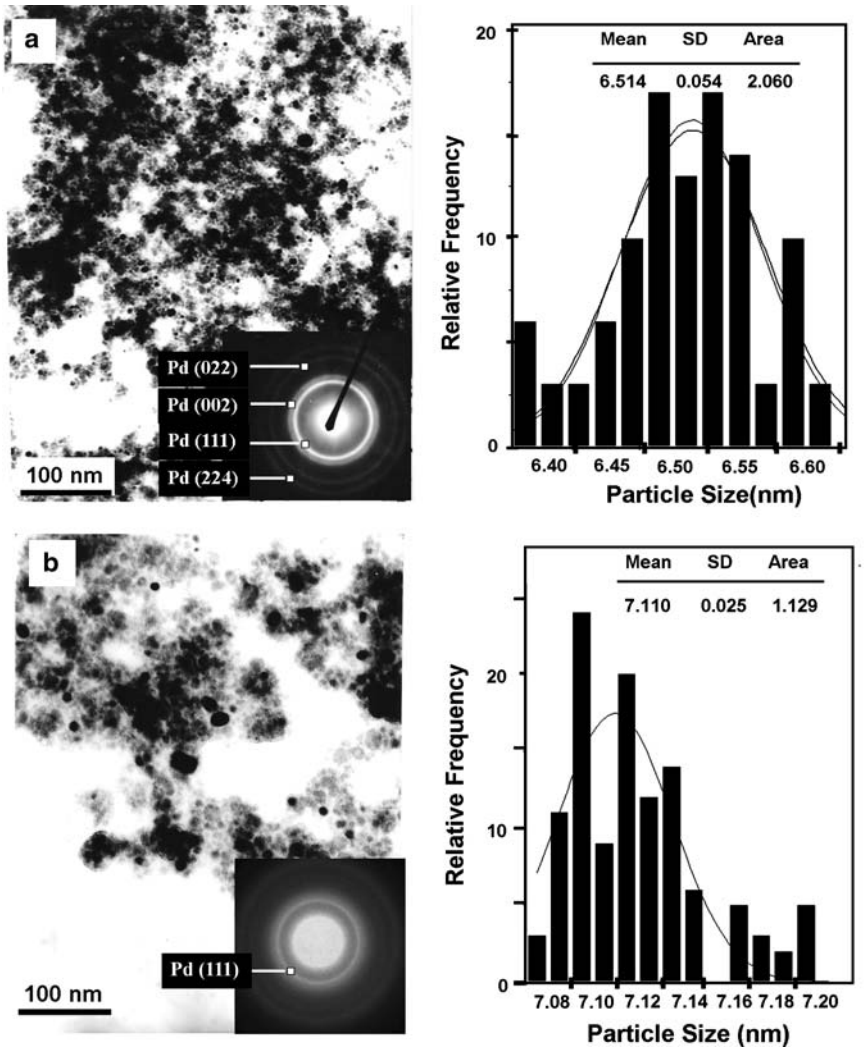


**Fig. 2** TEM micrographs, SAED and histograms for: **a** Pd-Coll-2-propanol ($1.43 \times 10^{-4}$ mol/L). **b** Pd-Coll-Styrene ($1.43 \times 10^{-4}$ mol/L)

process, producing this phenomenon. With the purpose of differentiating between fractal aggregates of Pd-Nps and the $TiO_2$ particles, Fig. 4e shows the electron diffraction pattern of anatase $TiO_2$ obtained with an aperture size of 50 nm. In this pattern we observed two rings with 3.52 and 1.89 Å, corresponding to the phase $TiO_2$ anatase (101) and (200), respectively.

Pd-Nps and ($Pd/TiO_2$) incorporation into PS matrix increased the decomposition temperature ($T_D$) of the Ncs. Table 3 and Fig. 5 summarize the ($T_D$) for the studied systems. On comparing the NCs-1 (0.1 mol% de AIBN), an increase of 5 °C on thermal stability was seen in contrast to PS (0.1 mol% AIBN). These NCs only

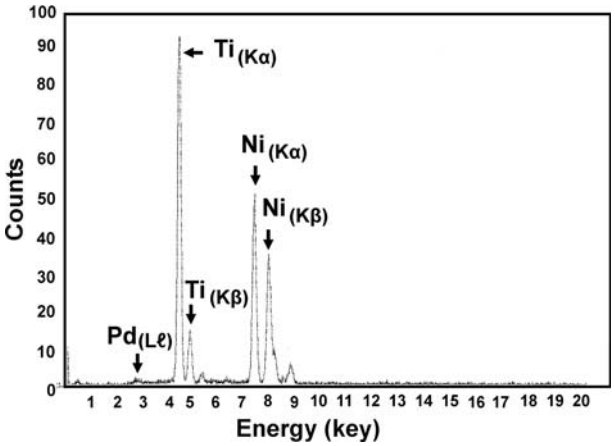


**Fig. 3** EDX of Pd/$TiO_2$/Styrene

**Table 2** Yielding percentage and average viscosimetric molecular weight % for the synthesized nanocomposites (Ncs)

| Nomenclature | Nanocomposite | AIBN (mol%) | Molar ratio (Pd/$TiO_2$) | Yield (%) | Mv ($10^4$) |
|---|---|---|---|---|---|
| | PS | 0.1 | – | 96.4 | 13.83 |
| | PS | 1.0 | – | 94.7 | 11.57 |
| Ncs-1 | PS/Pd | 0.1 | – | 88.0 | 12.96 |
| Ncs-2 | PS/Pd | 1.0 | – | 86.5 | 9.14 |
| Ncs-3 | PS/(Pd/$TiO_2$) | 0.1 | 1.0 | 87.3 | 9.73 |
| Ncs-4 | PS/(Pd/$TiO_2$) | 1.0 | 1.0 | 88.2 | 7.03 |
| Ncs-5 | PS/(Pd/$TiO_2$) | 0.1 | 5.0 | 85.9 | 9.10 |
| Ncs-6 | PS/(Pd/$TiO_2$) | 1.0 | 5.0 | 90.4 | 6.60 |

contain Pd-Nps. The Pd/$TiO_2$ rate increase produced a stability increase due to the presence of large amounts of thermically stable particles in the polymeric matrix. In this case, the decomposition temperature was 556, 10 °C more than the PS. The same trend in the increase of the $T_D$ were obtained to incorporate at PS: carbon nanotubes [27], $Fe_2O_3$ [35] and $TiO_2$ [36]. In most cases, Ncs obtained in the presence of thermically stable materials in a polymeric matrix are more stable than the raw polymer.

Thermal diffusivity ($\alpha$) values were determined by photoacoustic property evaluation and they are summarized in Table 4. Values of ($\alpha$) for PS with the NCs-1 and NCs-2 corresponding to Pd/PS (1%)–AIBN (0.1%) and AIBN (1.0%), respectively, and for NCs-3 (Pd/$TiO_2$) (1%)–AIBN (0.1%). Pd-Nps increase the thermal diffusivity of Ncs in comparison to the PS without nanoparticles, the latter showed ($\alpha$) 0.062 $cm^2/s$ and with Pd-Nps, the value was 0.155 $cm^2/s$. This increase of thermal diffusivity can be explained due to the increase of metallic nanoparticles

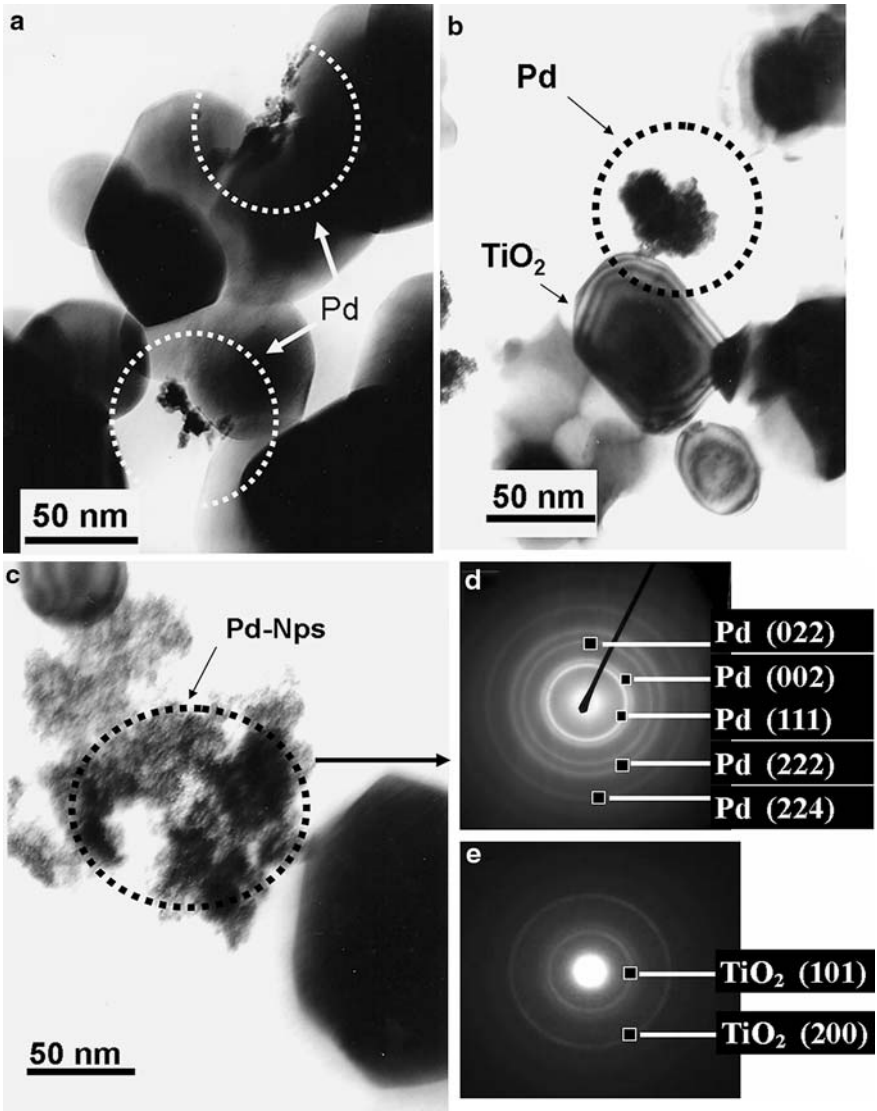


**Fig. 4** TEM micrographs **a** NCs-3, **b** NCs-4, **c** NCs-5, **d** SAED NCs-4, **e** $TiO_2$ (anatase) used in the synthesis

in the polymeric matrix, which shows good thermal conductive properties. Nanoparticles form energy conduction nuclei, facilitating the heat transfer of material by vibrations, translations and rotations of polymer chains close to metallic particles. When Pd/$TiO_2$ sensor particles are aggregated, thermal diffusivity decreases in contrast to NCs-1 and NCs-2, because the semiconductors oxides do not show good thermal conductivity as the metals. We considered that the particles shown in Fig. 4 are in direct contact due to the decrease in the thermal diffusivity of

**Table 3** Decomposition temperature ($T_D$) of studied Ncs

| Nanocomposite | $T_D$ (°C) | Weight loss (%) |
|---|---|---|
| PS (0.1 mol% AIBN) | 446.57 | 95.44 |
| PS (1 mol% AIBN) | 444.32 | 97.65 |
| Ncs-1 | 450.48 | 99.6 |
| Ncs-2 | 448.06 | 99.8 |
| Ncs-3 | 452.45 | 99.3 |
| Ncs-4 | 450.48 | 99.4 |
| Ncs-5 | 456.40 | 98.4 |
| Ncs-6 | 453.8 | 97.6 |

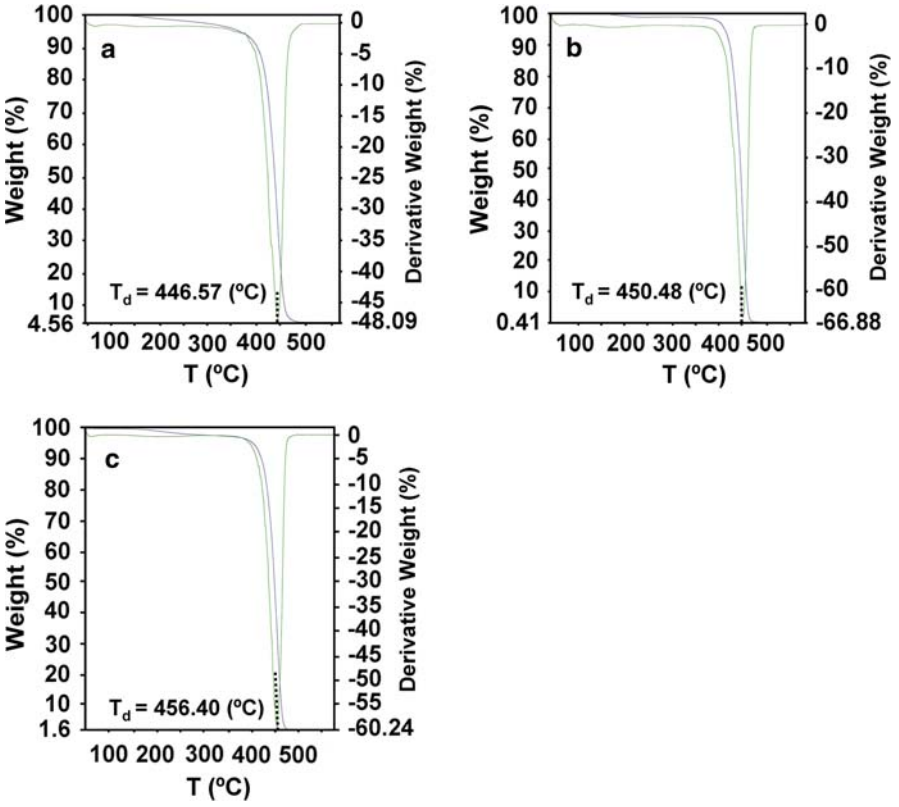


**Fig. 5** Thermograms for A: **a** PS (0.1 mol %AIBN), **b** NCs-1, **c** NCs-5

these Ncs. If it were otherwise, then both the fractal aggregate of Pd-Nps and Pd-Nps without aggregate distributed homogeneously by polymeric matrix would increase the thermal diffusivity of the materials to values close to those obtained for the NCs-1 and NCs-2.

**Table 4** Thermal diffusivity of the NCs obtained by photoacoustic

| Nanocomposites | Thickness (cm) ± 0.001 | Thermal diffusivity ($cm^2/s$) |
|---|---|---|
| PS | 0.058 | 0.062 ± 0.014 |
| Ncs-1 | 0.061 | 0.155 ± 0.012 |
| Ncs-2 | 0.079 | 0.157 ± 0.003 |
| Ncs-3 | 0.060 | 0.097 ± 0.006 |

The materials that adjusted their temperature more quickly to their surroundings were the NCs with metallic nanoparticles and those which had the least ($\alpha$) were the NCs with sensor particles and finally the polystyrene matrix.

## Conclusions

Pd-Nps and Pd/$TiO_2$ incorporation in the PS matrix increases the $T_D$ of Ncs, however, their MW are relatively similar.

Thermal diffusivity of Ncs is increased with the nanostructured material amount on a polymeric matrix. NCs with Pd-Npd had the best diffusivity due to good Pd thermal properties, which facilitate the heat transfer process of the matrix.

Styrene colloids are relatively stable and they have a strong trend to agglomerate in the polymerization and can be incorporated in the titanium oxide by SMAD method in situ producing, composite material with good particle distribution.

**Acknowledgments** We are grateful to CONICYT (AT-24071064; 21050655), AGCI and CIPA for scholarship grants. Sincere thanks are also given to Mecesup Project UCHO (Beca reforzamiento de la red nacional de programas de doctorado), Graduate School of Universidad de Concepción, FONDECYT 1040456 and Innova Bío-Bío for the financial support. Thanks to Nicola Bernard for her contribution to this work.

## References

1. Min KD, Kim MY, Choi KY, Lee JH, Lee SG (2006) Polym Bull 57:101
2. Huang HH, Wilkes GL (1987) Polym Bull 18:455
3. Noell JLW, Wilkes GL, Mohanty DK, McGrath JE (1990) J Appl Polym Sci 40:1177
4. Zhu Y, Sun DX (2004) J Appl Polym Sci 92:2013
5. LeBaron PC, Wang Z, Pinnavia T (1999) J Appl Clay Sci 15:11
6. Messersmith PB, Giannelis EP (1995) J Polym Sci Part A Polym Chem 33:1047
7. Wang MS, Pinnavia TJ (1994) Chem Mater 6:468
8. Vaia RA, Jandt KD, Kramer J, Giannelis EP (1995) Macromolecules 28:8080
9. Vaia RA, Ishii H, Giannelis EP (1995) Chem Mater 5:1694
10. Vaia RA, Vasudevan J, Krawie W, Scanlan LG, Giannelis EP (1995) Adv Mater 7:154
11. Wu W, He TB, Chen JF, Zhang XQ, Chen YX (2006) Mater Lett 60:2410
12. Du ZG, Zhang W, Zhang C, Jing ZH, Li HQ (2002) Polym Bull 49:151
13. Hasegawa H, Arai K, Saito S (1987) J Polym Sci Part A Polym Chem 25:3117
14. Hasegawa H, Arai K, Saito S (1987) J Polym Sci Part A Polym Chem 25:3231
15. Cárdenas G, Salgado E, Vera V (1996) Macromol Rapid Commun 17:775
16. Cárdenas G, Acuña J, Carbacho H, Rodríguez M (1994) Intern J Polymeric Mater 26:199
17. Cárdenas G, Salgado E (1997) Intern J Polymeric Mater 35:51

18. Cárdenas G, Salgado E (1997) Polym Bull 38:279
19. Godovsky D (2000) Adv Polym Sci 153:163
20. Sanchez C, Ribot F, Lebeau B (1999) J Mater Chem 9:35
21. Law H, Tou T (1998) Appl Opt 37:5694
22. Roth C, Kobrich R (1998) J Aerosol Sci 19:939
23. Greaves MD, Rotello VM (1997) J Am Chem Soc 119:10569
24. Huang QR, Kim HC, Huang E, Mecerreyes D, Hedrick JL, Volksen W, Frank CW, Miller RD (2003) Macromolecules 36:7661
25. Brongersma ML, Hartman JW, Atwater HA (2000) Phys Rev B 62:16356
26. Davies R, Schurr GA, Meenan P, Nelson RD, Bergna HE, Brevett CAS, Goldbaum RH (1998) Adv Mater 10:1264
27. Kim ST, Choi HJ, Hong SM (2007) Colloid Polym Sci 285:593
28. Yasnaya MA, Yu Kornilov, Sytnikov EV, Sinel'nikov BM, Kargin NI, Khoroshilova SE (2008) Inorg Mater 44:230
29. Zhang F, Zhang H, Su Z (2008) Polym Bull 60:251
30. Wang Z, Li G, Peng H, Zhang Z (2005) J Mater Sci 40:6433
31. Poussiganol P, Ricard D, Lucasik J, Flytzanis C (1987) J Opt Soc Am B 4:5
32. Flytzanis C, Hache F, Klein MC, Richard D, Poussiganol P (1991) Progr Opt 29:323
33. Wang J, Montville D, Gonsalves KE (1999) J Appl Polym Sci 72:1852
34. Sreekumari Nair P, Radhakrishnan T, Revaprasadu N, Kolawole GA (2005) J Mater Sci 40:4407
35. Kuljanin J, Marinovic-Cincovic M, Zec S, Comor MI, Nedeljkovic JM (2003) J Mater Sci 22:235
36. Jang LB, Sung JH, Choi HJ, Chin I (2005) J Mater Sci 40:3021
37. Lima CAS, Oliva R, Cárdenas G, Silva EN, Miranda LCM (2001) Mater Lett 51:357
38. Cárdenas G, Oliva R, Reyes P, Rivas B (2003) J Mol Catal A Chem 191:75
39. Billmeyer FW (1962) Textbook of polymer science, 2nd edn. Wiley, New York, p 290
40. Bandrup J, Immegut GH (eds) (1998) Polymer handbook 3rd edn. Wiley, New york, pp VII-19; II-205
41. Lima CAS, Lima MBS, Oliva R, Cárdenas G, Miranda LCM (2000) Chem Phys Lett 332:428
42. Meléndrez MF, Cárdenas C, Díaz J, Cruzat C, Arbiol J (2008) Colloid Polym Sci. doi: 10.1007/s00396-008-1950-7
43. Segura R, Reyes-Gasca J, Cárdenas G (2005) Colloid Polym Sci 283:854
44. Cárdenas G, Muñoz C, Rodriguez M, Morales J, Soto H (1999) Eur Polym J 35:1017
45. Cárdenas C, González M (1996) Inter J Polymeric Mater 34:169
46. Klabunde KJ, Cárdenas C (1996) Metal atom/vapor approaches to active metal cluster/particles. VCH, New York, p 237
47. Powder diffraction File, Inorganic Phases, JCPDS (1997) International Centre for Diffraction data, USA